

Electronic Supplementary Information

Morphological and Surface Structural Evolutions of MgO Particles from Parallelograms to Rods

Yajun Zheng,^[†] Xiaoling Zhang,^[†] Xuan Wang, Qian Wang, Zongquan Bai, and Zhiping Zhang*

School of Chemistry and Chemical Engineering, Xi'an Shiyou University, Xi'an 710065, China

Fax: (+86) 29-8838-2693

E-mail: zhangzp0304@gmail.com (Z. Zhang)

^[†] These authors contributed equally to this work.

Experimental

1. Materials

Magnesium nitrate ($\text{Mg}(\text{NO}_3)_2 \cdot 6\text{H}_2\text{O}$), sodium oxalate ($\text{Na}_2\text{C}_2\text{O}_4$), potassium carbonate (K_2CO_3) and benzaldehyde were purchased from Tianjin Fu Chen Chemical Reagents Factory (Tianjin, China). Absolute ethanol was from Tianjin Tianli Chemical Reagents Co. (Tianjin, China).

2. Synthesis of trapezoid-liked and rod-liked MgO particles

The procedures for preparation of trapezoid-like and rod-like MgO micro-particles were similar to the previous reports.^{1,2} In a typical procedure, 10.26 g $\text{Mg}(\text{NO}_3)_2 \cdot 6\text{H}_2\text{O}$ (0.04 mol) was dissolved into 50 mL of double-deionized water. Then, the $\text{Mg}(\text{NO}_3)_2$ solution was transferred to a 250 mL three-necked flask and heated to 50 °C. Subsequently, 0.04 mol $\text{Na}_2\text{C}_2\text{O}_4$ or K_2CO_3 was dissolved into 100 mL of double-deionized water, and then the $\text{Na}_2\text{C}_2\text{O}_4$ or K_2CO_3 solution was also heated to 50 °C. Under a vigorous stirring (ca. 800 rpm), the $\text{Na}_2\text{C}_2\text{O}_4$ or K_2CO_3 solution was poured into the $\text{Mg}(\text{NO}_3)_2$ solution in 4-5 s. The mixture was further stirred for 1 min and then maintained at the temperature of 50 °C under static conditions for 1 hour. Then collected the white precipitate, filtered off, and washed with double-deionized water and absolute ethanol several times, respectively. Finally, the obtained product was dried at 70 °C for several hours. After that, the dried powder was calcined in air from room temperature to 300 °C with a rate of 1 °C min^{-1} followed by maintaining for 2 h and, and finally the resulting product was calcined at 550 °C in a muffle furnace for 3 h.

3. Synthesis of MgO particles from the precipitation reactions of $\text{Mg}(\text{NO}_3)_2$ in the presence of various ratios of $\text{Na}_2\text{C}_2\text{O}_4$ to K_2CO_3

The major synthesis procedures for preparing the samples were similar to those described above except that the pure $\text{Na}_2\text{C}_2\text{O}_4$ or K_2CO_3 solution was replaced by the mixed basic precipitation reagent $\text{Na}_2\text{C}_2\text{O}_4$ (0.0356, 0.0320, 0.0267, 0.020, 0.0133, 0.0080, 0.0044 mol) and K_2CO_3 (0.0044, 0.0080, 0.0133, 0.020, 0.0267, 0.0320, 0.0356 mol) with molar ratios of 8:1, 4:1, 2:1, 1:1, 1:2, 1:4 and 1:8 ($\text{Na}_2\text{C}_2\text{O}_4/\text{K}_2\text{CO}_3$) in 100

mL double-deionized water.

4. Samples Characterization

The crystal structures of the as-synthesized products were characterized by X-ray diffraction (XRD) on a XRD-6000 diffractometer using Cu K α radiation. The operation voltage was 40 kV, and the current was 30 mA. The morphology, size and energy dispersive spectra (EDS) of the obtained particles were examined by a JEOL JSM-6390A scanning electron microscope (SEM). The thermal decomposition behaviors of the MgO precursors were detected by a thermogravimetric analyzer (TGA, Mettler Toledo, TGA/DSC1 STAR System, Switzerland), which was carried out in dynamic nitrogen gas with a heating rate of 10 °C min⁻¹. The N₂ adsorption-desorption isotherm was determined on a Micromeritics ASAP 2020HD88 instrument physisorption apparatus at the temperature of liquid nitrogen, in which the samples were degassed at 350 °C for 4 h before measurement. The surface area was calculated by the Brunauer-Emmett-Teller method. Temperature-programmed desorption of CO₂ (CO₂-TPD) was carried out to determine the basicity of the MgO particles using a Micromeritics ChemiSorb 2750 reactor. In the process, 600 mg MgO was heated to 300 °C at a rate of 10 °C min⁻¹ under an Ar gas flow (50 ml min⁻¹) and maintained at that temperature for 2 h to remove the surface impurities. After cooling down to 50 °C under an Ar gas flow (50 ml min⁻¹), the sample was exposed to CO₂ atmosphere (50 ml min⁻¹) for 3.5 h. Thereafter, the sample was purged with He gas (50 ml min⁻¹) for 1.5 h and then heated to 800 °C at a rate of 10 °C min⁻¹.

5. Catalytic evaluation

The catalysts were evaluated by using the MPV reaction between ethanol and benzaldehyde. In a typical reaction, ethanol (17.5 mL, 300 mmol), benzaldehyde (1.5 mL, 15 mmol), and as-synthesized MgO (2.5 g) were transferred into a 50 mL round-bottom flask equipped with a reflux condenser. The reaction mixture was heated to the reflux temperature (78 °C) under magnetic stirring. The reaction solution was withdrawn in different intervals by using a micropipette during the reaction. The collected products were analyzed with an Agilent GC-7890B gas chromatograph

equipped with a HP-INNOWax capillary column (30 m × 0.32 mm I.D., 0.25 μm film thickness).

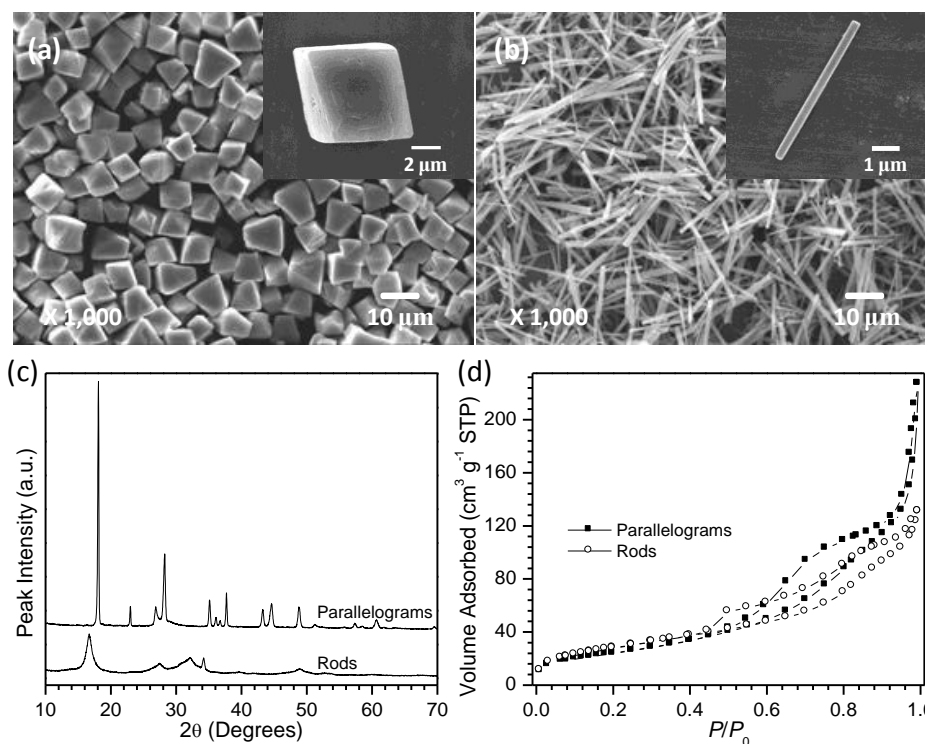


Figure S1. SEM images of a) parallelogram-like particles constructed from Mg²⁺ and C₂O₄²⁻, and rod-like particles constructed from Mg²⁺ and CO₃²⁻; c) PXRD patterns of parallelogram-like particles (top) and rod-like particles (bottom); d) N₂ adsorption isotherms of parallelogram-like MgO particles (solid square) and rod-like MgO particles (hollow circle) by heating their corresponding precursors at 550 °C.

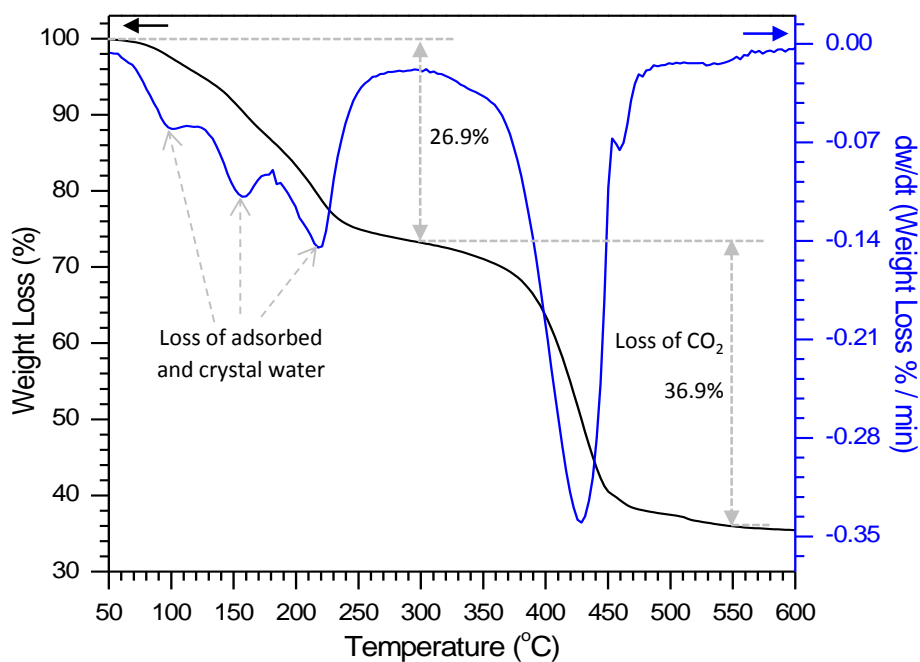


Figure S2. Thermogravimetric (TG) and thermogravimetric derivative (DTG) curves of the resulting rod-like particles by reaction between $\text{Mg}(\text{NO}_3)_2$ and K_2CO_3 at 50 °C. (Note: The approximate molecular formula was calculated based on the weight losses of water, CO_2 as well as the remaining MgO after calcination, and a close formula of $\text{MgCO}_3 \cdot 0.7\text{H}_2\text{O}$ was obtained.)

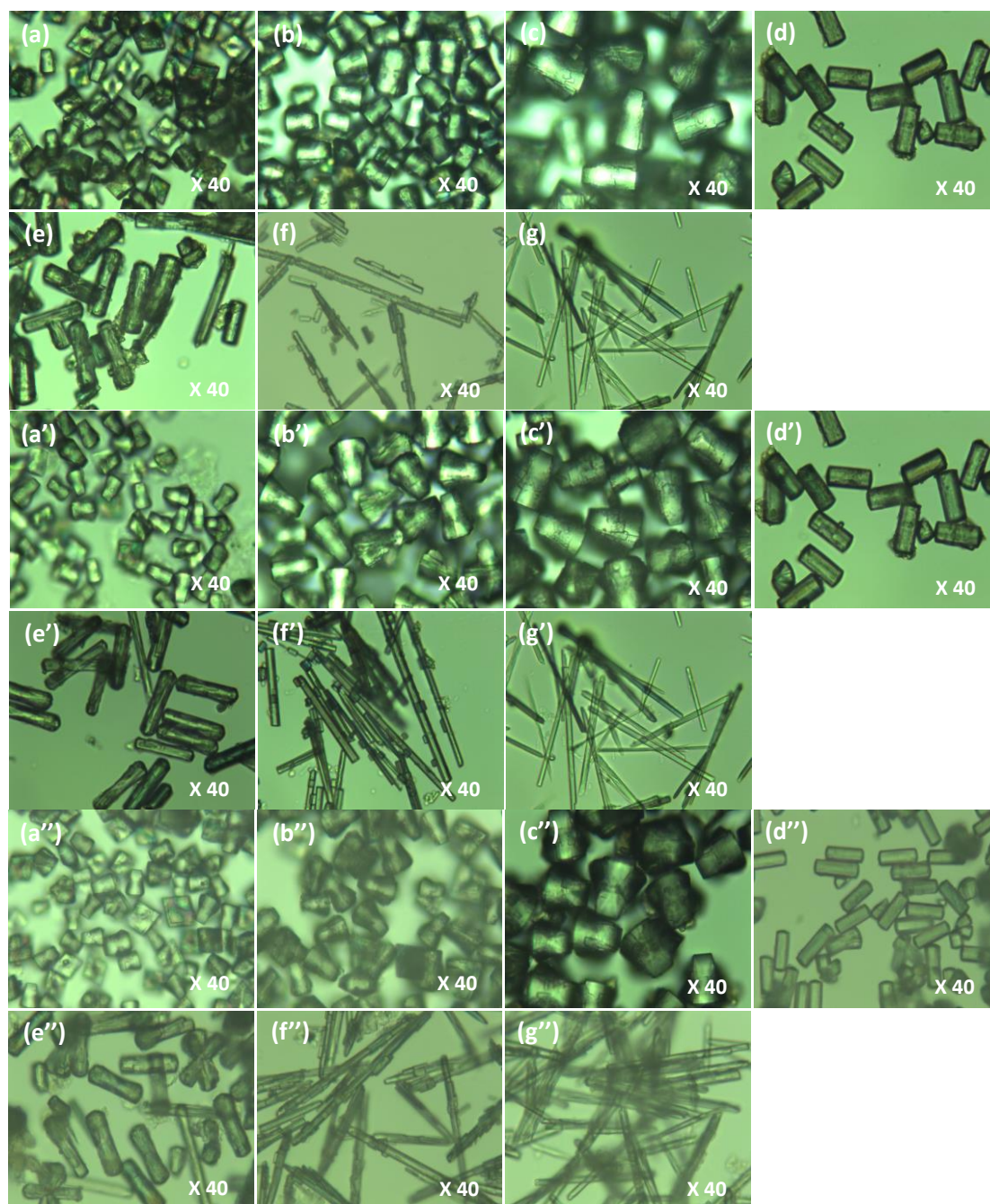


Figure S3. Photographic images exhibiting the morphological evolution of MgO precursors constructed from the precipitation reaction of $\text{Mg}(\text{NO}_3)_2$ in the presence of various ratios of a-g) $\text{Na}_2\text{C}_2\text{O}_4$ to K_2CO_3 , a'-g') $\text{K}_2\text{C}_2\text{O}_4$ to K_2CO_3 a''-g'') $\text{Na}_2\text{C}_2\text{O}_4$ to Na_2CO_3 at 50 °C. The ratios of $\text{C}_2\text{O}_4^{2-}/\text{CO}_3^{2-}$ (mol/mol) employed during the reactions were a) 8:1, b) 4:1, c) 2:1, d) 1:1, e) 1:2, f) 1:4 and g) 1:8.

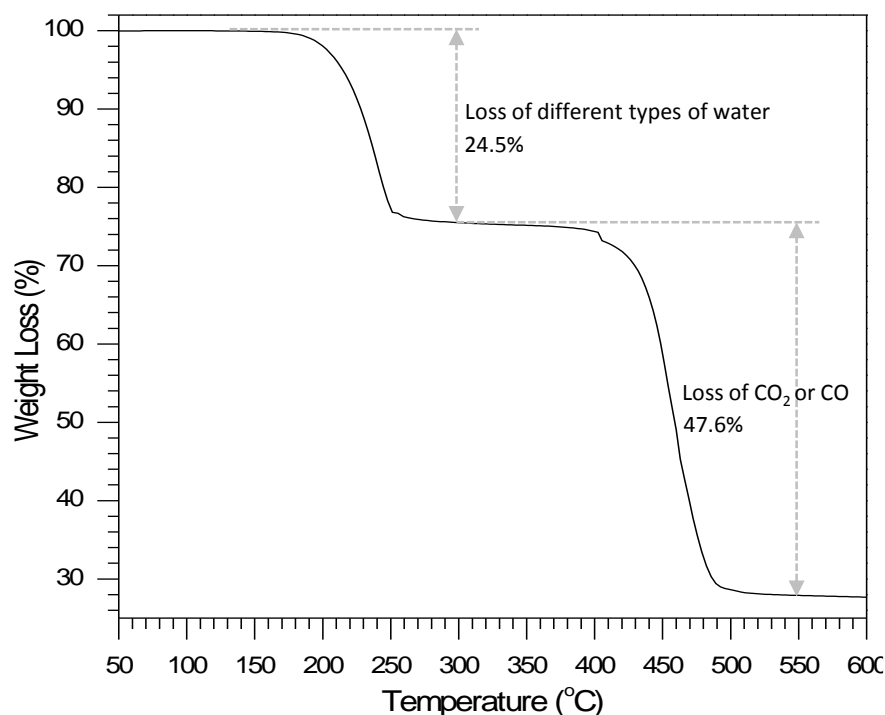


Figure S4. Thermogravimetric (TG) curve of the resulting product by reaction between $\text{Mg}(\text{NO}_3)_2$ and $\text{Na}_2\text{C}_2\text{O}_4/\text{K}_2\text{CO}_3$ with a theoretical ratio of 8:1 at 50 °C.

Figure S4 shows a typical TG curve of the resulting product by reaction between $\text{Mg}(\text{NO}_3)_2$ and $\text{Na}_2\text{C}_2\text{O}_4/\text{K}_2\text{CO}_3$ with a theoretical molar ratio of 8:1 at 50 °C. According to the previous reports,³⁻⁷ the sample mass decreased from 50 to 300 °C due to the elimination of different types of absorbed or crystal water, and with increase in the temperature from 300 to 550 °C, these samples exhibited a significant mass drop due to the elimination of $\text{C}_2\text{O}_4^{2-}$ or/and CO_3^{2-} as the form of CO_2 or/and CO . Above the temperature of 550 °C, the products kept as the form of MgO . According to the above discussion, the product existed as the form of MgC_2O_4 and MgCO_3 at the temperature of 300 °C, and above 550 °C MgO was the sole form. Based on this fact, we can assume that there is x mole MgC_2O_4 and y mole MgCO_3 . Because we know the molecular weights of MgC_2O_4 (112.3240 g/mol), MgCO_3 (84.3139 g/mol) and MgO (40.3044 g/mol) and the mass at 300 °C (75.48%) and 550 °C (27.89%), the following equations could be derived.

$$112.3240x + 84.3139y = 0.7548 \quad (1)$$

$$40.3044(x + y) = 0.2789 \quad (2)$$

From Equations (1) and (2), x and y could be obtained, namely $x = 6.118 \times 10^{-3}$, $y = 8.020 \times 10^{-4}$.

Therefore, $x:y = 6.118 \times 10^{-3}/8.020 \times 10^{-4} = 7.63:1$

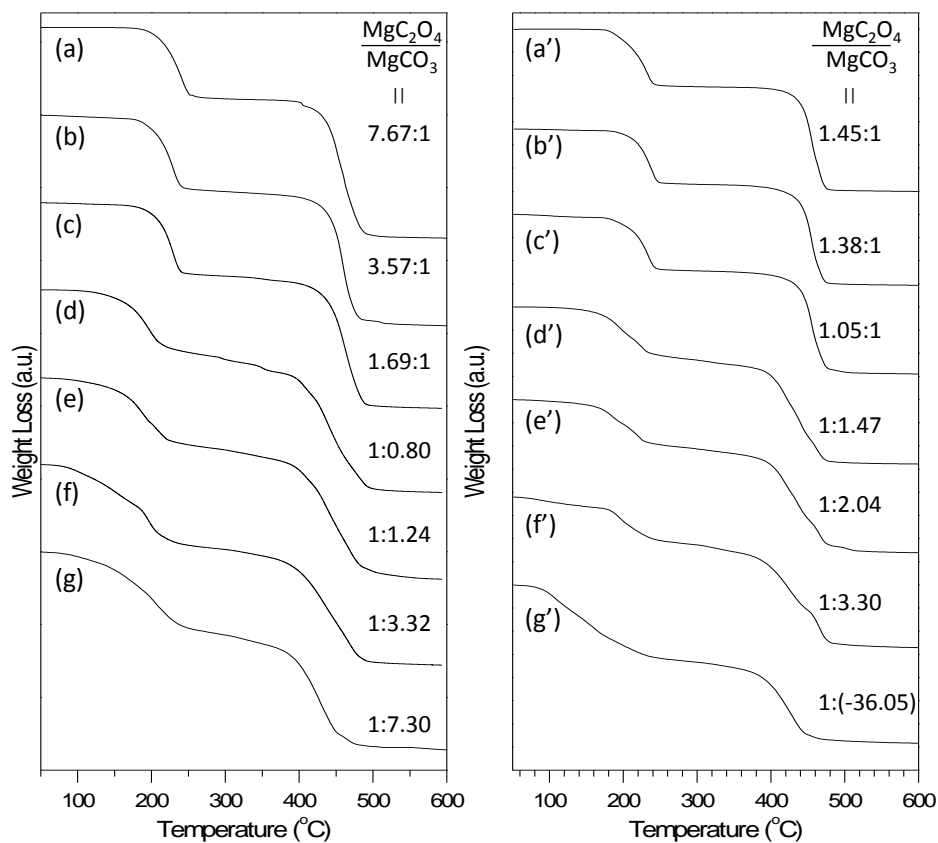


Figure S5. Thermogravimetric (TG) curves of differently shaped MgO precursors, in which the ratios of a-g) $\text{Na}_2\text{C}_2\text{O}_4$ to Na_2CO_3 (mol/mol) and a'-g') $\text{K}_2\text{C}_2\text{O}_4$ to K_2CO_3 (mol/mol) employed during the reactions were a) and a') 8:1, b) and b') 4:1, c) and c') 2:1, d) and d') 1:1, e) and e') 1:2, f) and f') 1:4, and g) and g') 1:8.

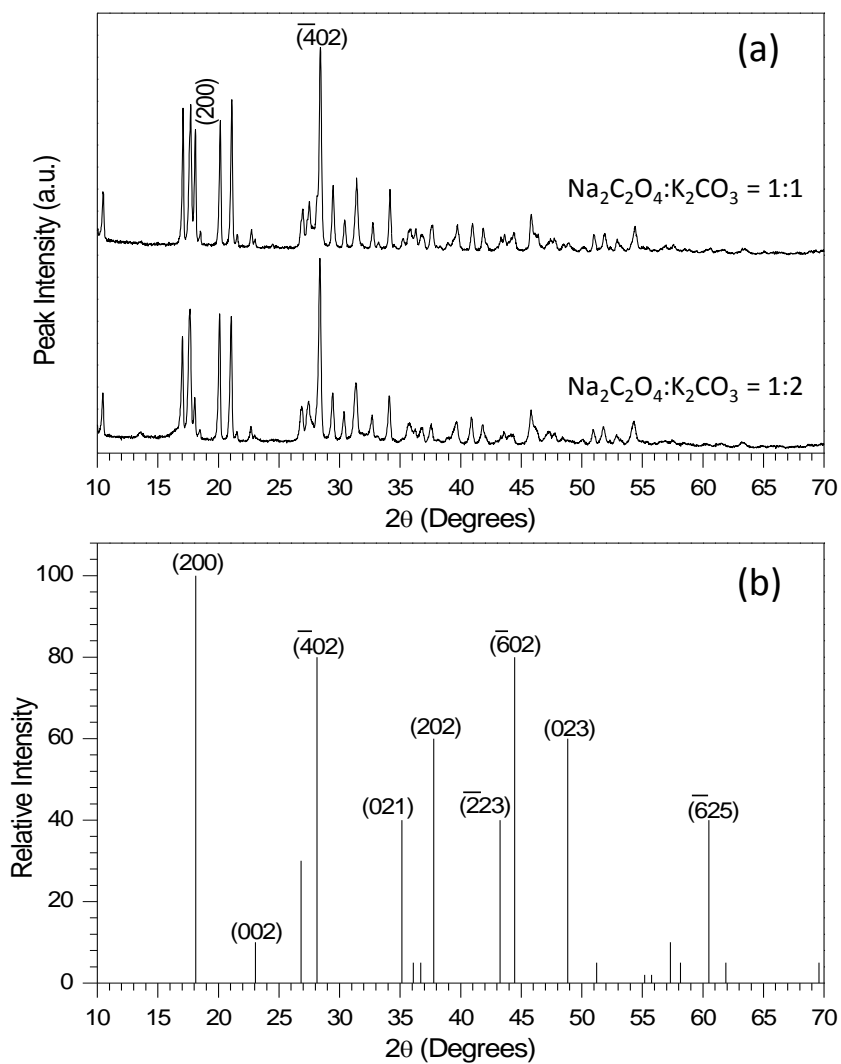


Figure S6. a) PXRD patterns of MgO precursors constructed from the precipitation reaction of $\text{Mg}(\text{NO}_3)_2$ in the presence of 1:1 and 1:2 of $\text{Na}_2\text{C}_2\text{O}_4$ to K_2CO_3 at 50°C ; b) Standard PXRD pattern of $\text{MgC}_2\text{O}_4 \cdot 2\text{H}_2\text{O}$ (JCPDS No.: 28-0625).

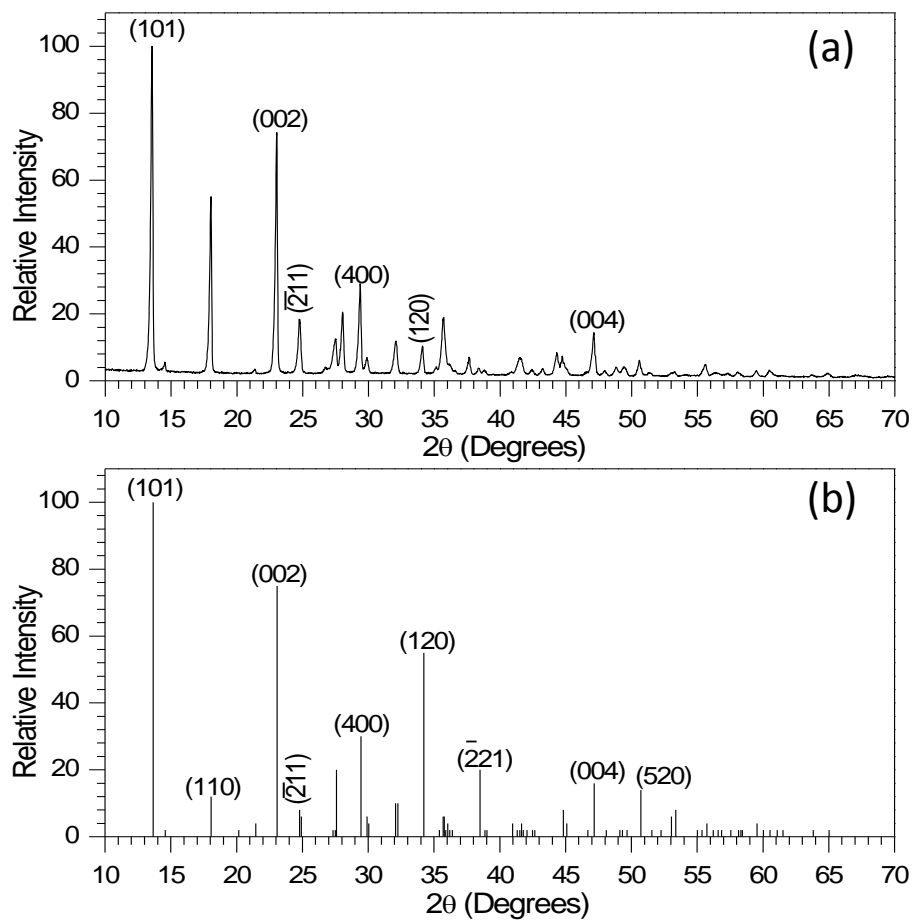


Figure S7. a) XRD patterns of MgO precursors constructed from the precipitation reaction of $\text{Mg}(\text{NO}_3)_2$ in the presence of 1:4 of $\text{Na}_2\text{C}_2\text{O}_4$ to K_2CO_3 at 50°C ; b) Standard XRD pattern of $\text{MgCO}_3 \cdot 3\text{H}_2\text{O}$ (JCPDS No.: 20-0669).

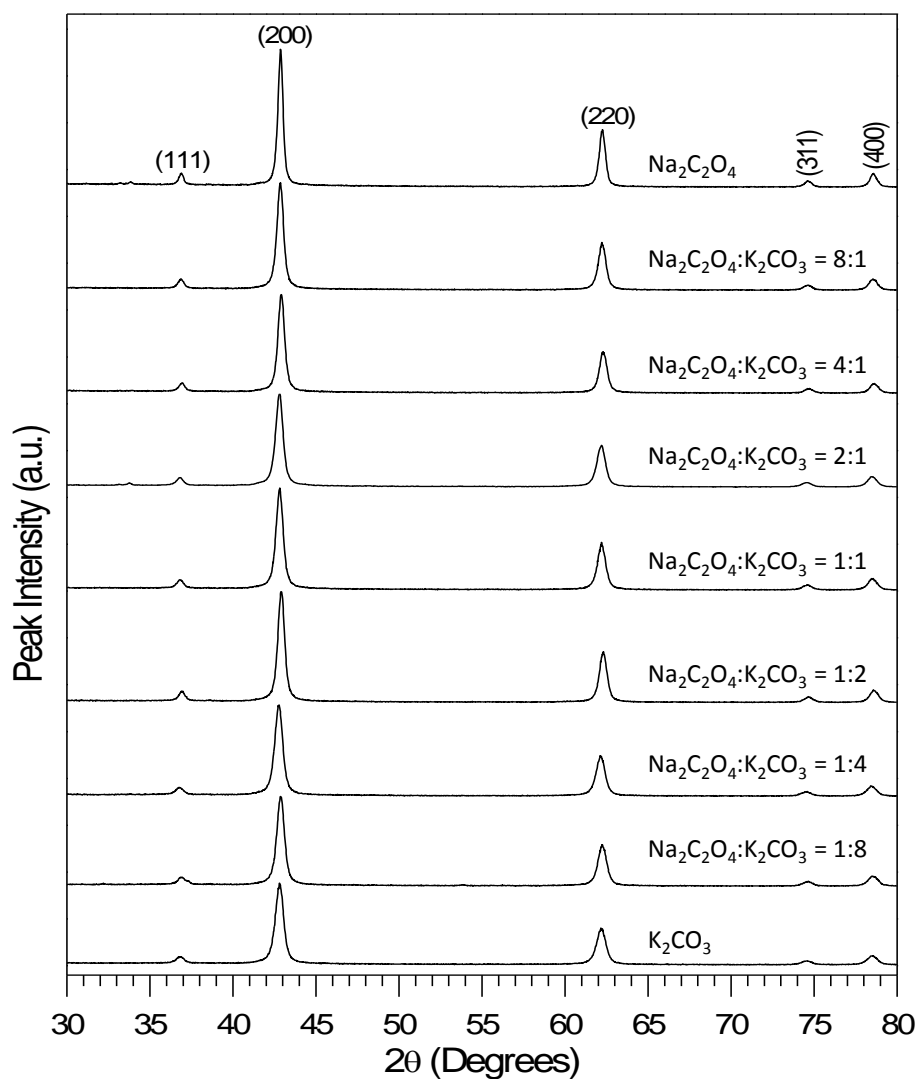


Figure S8. PXRD patterns of MgO by calcination of their precursors constructed from the precipitation reaction of $\text{Mg}(\text{NO}_3)_2$ in the presence of various ratios of $\text{Na}_2\text{C}_2\text{O}_4$ to K_2CO_3 as indicated in this figure (calcination temperature: 550°C).

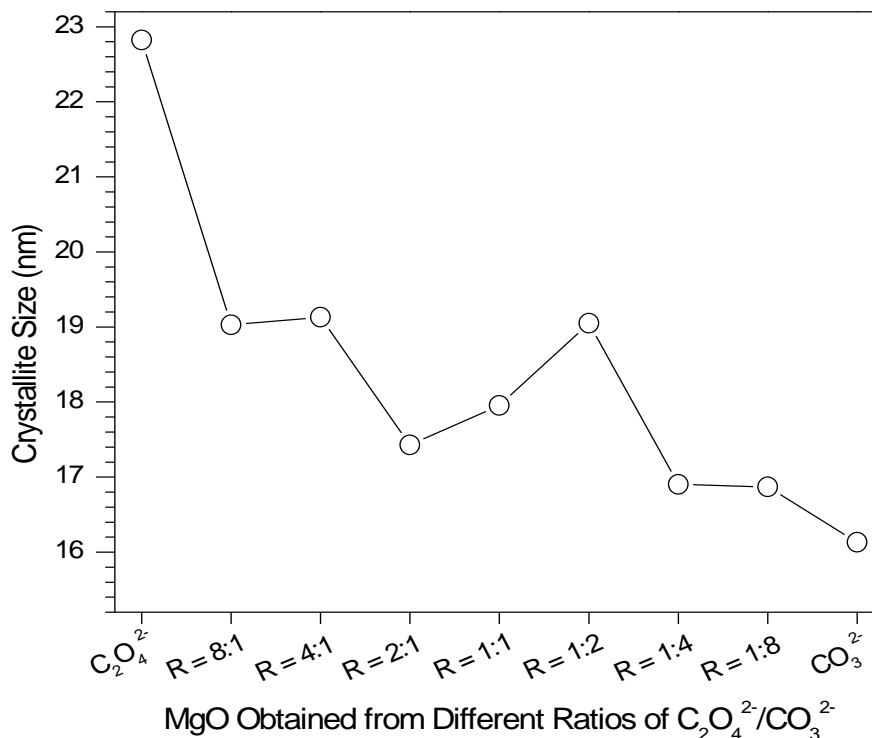


Figure S9. Variation of crystallite size from the PXRD patterns of MgO by calcination of their precursors constructed from the precipitation reaction of $Mg(NO_3)_2$ in the presence of various ratios of $Na_2C_2O_4$ to K_2CO_3 as indicated in this figure.

Note: Crystallite size was calculated from the Scherrer equation $D = (K \lambda) / (\beta \cos \theta)$, where D is the mean crystallite size of the ordered domains; K is a dimensionless shape factor (0.89 in the present study); λ is the X-ray wavelength (0.154056 nm); β is the line broadening at half the maximum intensity (FWHM); θ is the Bragg angle.

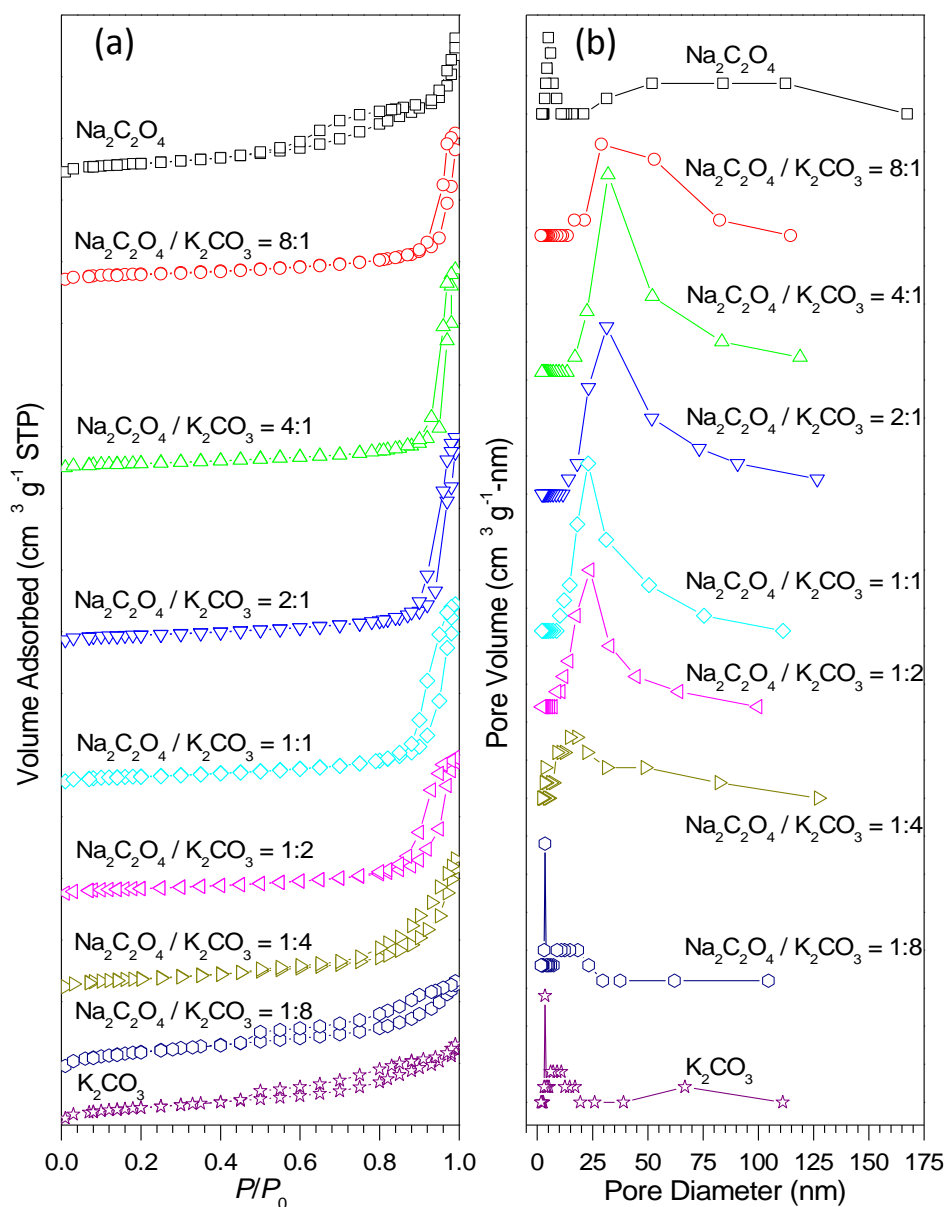


Figure S10. a) N₂ adsorption-desorption isotherms and their corresponding BJH pore size distribution curves of MgO particles by calcination of their precursors constructed from the precipitation reaction of Mg(NO₃)₂ in the presence of various ratios of Na₂C₂O₄ to K₂CO₃ as indicated in this figure.

Table S1. Texture properties of the obtained MgO by calcination of their precursors constructed from the precipitation reaction of $\text{Mg}(\text{NO}_3)_2$ in the presence of various ratios of $\text{Na}_2\text{C}_2\text{O}_4$ to K_2CO_3 .

| Ratio of $\text{Na}_2\text{C}_2\text{O}_4$ to K_2CO_3 | BET surface area ($\text{m}^2 \cdot \text{g}^{-1}$) ^[a] | Pore Volume ($\text{cm}^3 \cdot \text{g}^{-1}$) ^[b] | Average Pore Diameter (nm) |
|---|--|--|----------------------------|
| Pure $\text{Na}_2\text{C}_2\text{O}_4$ | 89.8 | 0.35 | 9.8 |
| 8:1 | 54.1 | 0.38 | 23.1 |
| 4:1 | 47.0 | 0.50 | 31.1 |
| 2:1 | 53.9 | 0.52 | 28.5 |
| 1:1 | 55.8 | 0.46 | 22.9 |
| 1:2 | 50.1 | 0.35 | 19.1 |
| 1:4 | 82.7 | 0.33 | 12.7 |
| 1:8 | 143.7 | 0.23 | 5.7 |
| Pure K_2CO_3 | 104.0 | 0.20 | 6.0 |

Note: ^[a] Using the standard Brunauer–Emmett–Teller (BET) method; ^[b] Using the Barret–Joyner–Halenda (BJH) method.

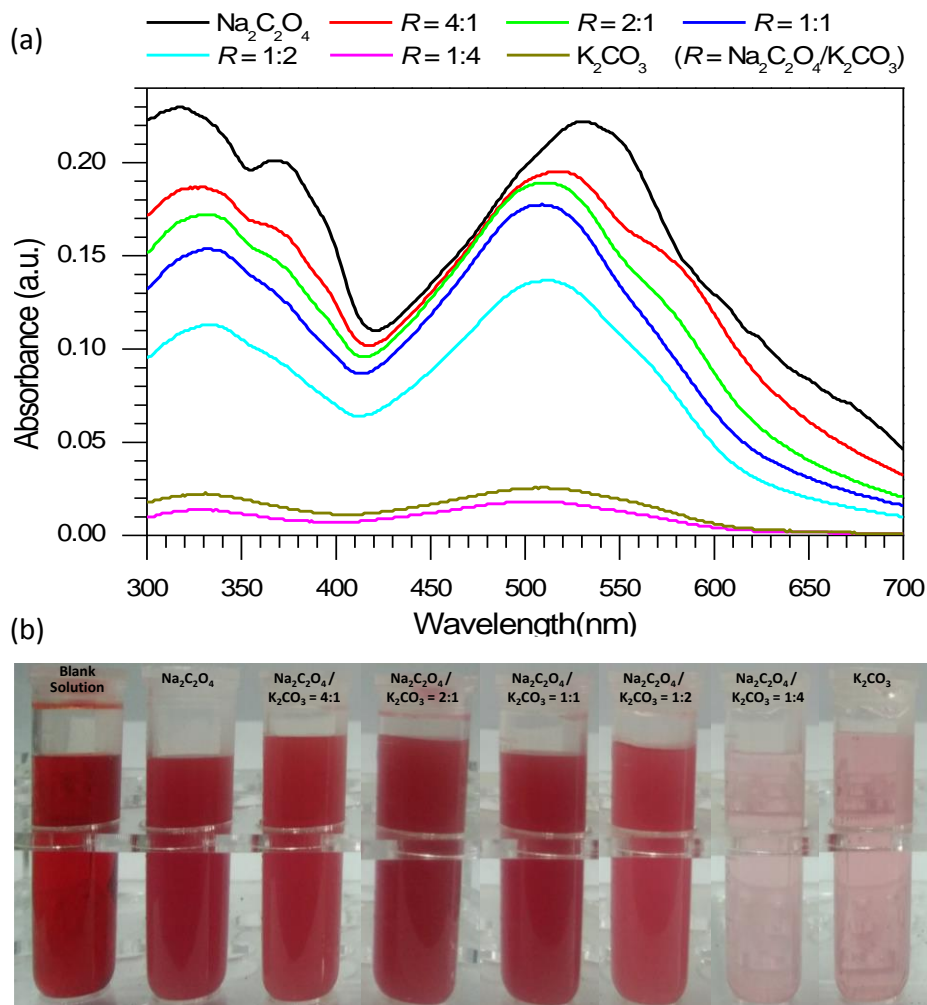


Figure S11. a) UV-vis spectra of Congo red aqueous solutions after being treated by different MgO particles by calcination of their precursors constructed from the precipitation reaction of $\text{Mg}(\text{NO}_3)_2$ in the presence of various ratios of $\text{Na}_2\text{C}_2\text{O}_4$ to K_2CO_3 as indicated in this figure, and b) photographic images of Congo red aqueous solution (Blank Solution, 200 mg L^{-1}) treated by as-prepared MgO particles as indicated. From this figure, it is obvious that the adsorption ability of these MgO particles varied with the ratio between $\text{Na}_2\text{C}_2\text{O}_4$ and K_2CO_3 . When the ratio between $\text{Na}_2\text{C}_2\text{O}_4$ and K_2CO_3 was 1:4, the resulting MgO demonstrated the superior adsorption ability to Congo red aqueous solution relative to others. The corresponding experiment is still under way and will be reported in due course.

Note: The adsorption experiments were carried out by mixing as-prepared MgO particles (10 mg) with 10 mL Congo red aqueous solution (200 mg L^{-1}) in a beaker (100 mL) under stirring at natural pH value and room temperature. After an adsorption time of 1 h, the mixture solutions were collected and separated through centrifugation. The concentrations of Congo red solutions in the filtrates were measured on Shimadzu UV-2600 UV-visible spectrophotometer.

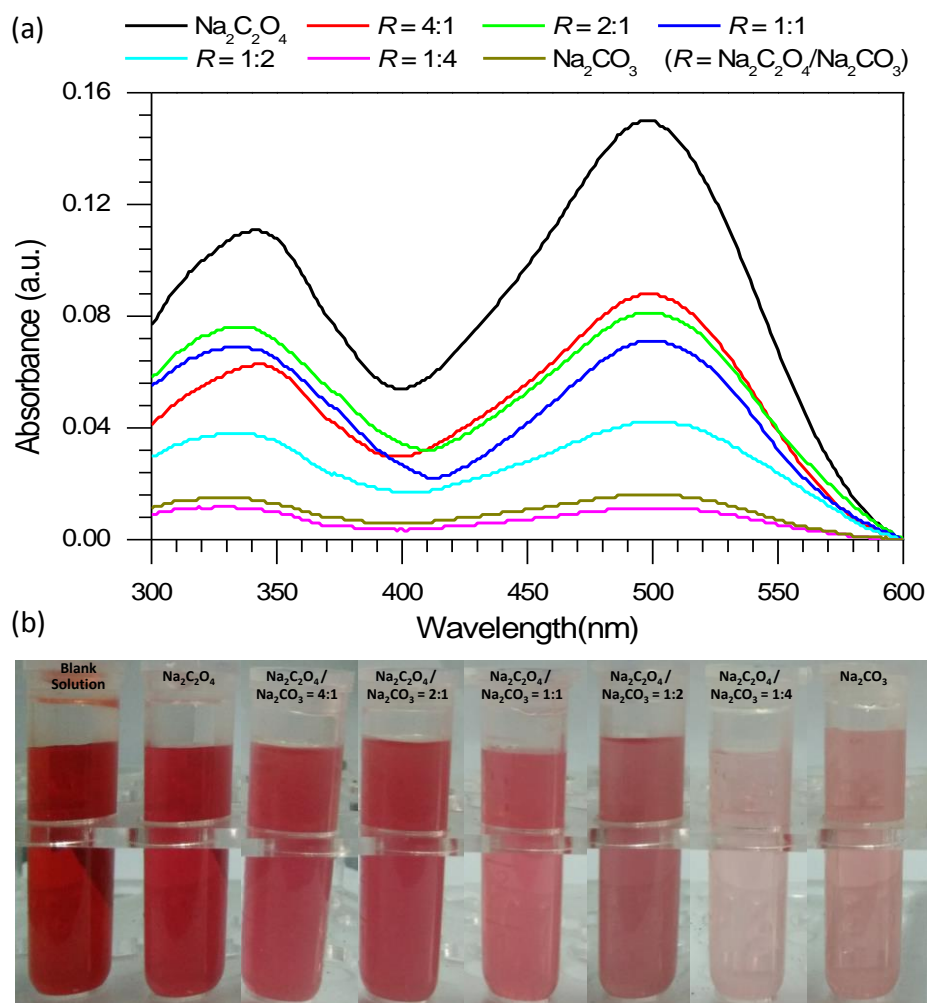


Figure S12. a) UV-vis spectra of Congo red aqueous solutions after being treated by different MgO particles by calcination of their precursors constructed from the precipitation reaction of $\text{Mg}(\text{NO}_3)_2$ in the presence of various ratios of $\text{Na}_2\text{C}_2\text{O}_4$ to Na_2CO_3 as indicated in this figure, and b) photographic images of Congo red aqueous solution (Blank Solution, 200 mg L^{-1}) treated by as-prepared MgO particles as indicated. From this figure, it is obvious that the adsorption ability of these MgO particles varied with the ratio between $\text{Na}_2\text{C}_2\text{O}_4$ and Na_2CO_3 . When the ratio between $\text{Na}_2\text{C}_2\text{O}_4$ and Na_2CO_3 was 1:4, the resulting MgO demonstrated the superior adsorption ability to Congo red aqueous solution relative to others.

In the present study, the as-synthesized porous MgO particles from different ratios of $\text{Na}_2\text{C}_2\text{O}_4$ to K_2CO_3 were used to adsorb Congo red (CR). Figure S11a shows the UV-vis absorption spectra of CR solutions after being treated by different MgO products with a fixed initial CR concentration of 200 mg L^{-1} . With variation of the ratio between $\text{Na}_2\text{C}_2\text{O}_4$ and K_2CO_3 , the removal efficiency of the CR demonstrated a first increasing trend followed by decreasing. When the ratio between $\text{Na}_2\text{C}_2\text{O}_4$ and K_2CO_3 was 1:4, the CR can be almost completely adsorbed, which was also supported by the color

change of the CR solution changing from deep red to almost colorless followed by deep red again (Figure S11b). From the present available primary data (data not shown), the adsorption capacities of Congo red by using the MgO from 1:4 Na₂C₂O₄/K₂CO₃ was 405 mg g⁻¹, which was much higher than those from MgO nanoplates (131 mg g⁻¹)⁸ but lower than those from porous hierarchical MgO (2409 mg g⁻¹).⁹ In addition, it should be pointed out that the cation species of the alkali for preparation of MgO precursors had little effect on the performance of the obtained MgO (Figure S12). The effects of experimental parameters on the adsorption capacities of Congo red by using the MgO from 1:4 Na₂C₂O₄/K₂CO₃ are still in investigation, and will be reported in due course.

References

1. Z. P. Zhang, Y. J. Zheng, Y. W. Ni, Z. M. Liu, J. P. Chen and X. M. Liang, *J. Phys. Chem. B*, 2006, **110**, 12969-12973.
2. X. Zhang, Y. Zheng, H. Yang, Q. Wang and Z. Zhang, *CrystEngComm*, 2015, **17**, 2642-2650.
3. Z. Zhang, Y. Zheng, J. Zhang, Q. Zhang, J. Chen, Z. Liu and X. Liang, *Crys. Growth Des.*, 2007, **7**, 337-342.
4. W. Zhu, L. Zhang, G.-L. Tian, R. Wang, H. Zhang, X. Piao and Q. Zhang, *CrystEngComm*, 2014, **16**, 308-318.
5. F. Mohandes, F. Davar and M. Salavati-Niasari, *J. Phys. Chem. Solids*, 2010, **71**, 1623-1628.
6. Z. Hao, J. Pan and F. Du, *Mater. Lett.*, 2009, **63**, 985-988.
7. R. L. Frost, M. Adebajo and M. L. Weier, *Spectrochim. Acta A*, 2004, **60**, 643-651.
8. J. Hu, Z. Song, L. Chen, H. Yang, J. Li and R. Richards, *J. Chem. Eng. Data*, 2010, **55**, 3742-3748.
9. P. Tian, X.-Y. Han, G.-I. Ning, H.-X. Fang, J.-W. Ye, W.-T. Gong and Y. Lin, *ACS Appl. Mater. Inter.*, 2013, **5**, 12411-12418.